DETERMINING THE FEASIBILITY OF MEASURING OUTDOOR ROAD CYCLING KINEMATICS USING INERTIAL MOTION CAPTURE TECHNOLOGY

J. Cockcroft* and C. Scheffer**

** Biomedical Engineering Research Group, Dept. of Mechanical and Mechatronic Engineering, Stellenbosch University, Stellenbosch, South Africa E-mail: johnc@sun.ac.za*
*** Biomedical Engineering Research Group, Dept. of Mechanical and Mechatronic Engineering, Stellenbosch University, Stellenbosch, South Africa E-mail: cscheffer@sun.ac.za*

Abstract: Unlike traditional optical systems, inertial motion capture systems (IMSs) can measure human kinematics outdoors as well as in a laboratory. However, these systems are sensitive to magnetic interference. This study evaluated an IMS for use in sports performance analysis, using road cycling as a case study. The objective was to establish the feasibility of obtaining accurate outdoor kinematic data on competition-level road bicycles. Ten male cyclists were recorded on their own bicycle on a stretch of road wearing the IMS. Results revealed unacceptable magnetic interference to the IMS near the pedal and handlebar interfaces. Therefore, accurate full-body cycling kinematics is not currently feasible on most competition-level road bicycles. However, lower limb flexion measurements are possible using the IMS's kinematic coupling algorithm which obtained RMS errors of less than 3.5° for all joints in a benchmark test with an optical system regarded as gold-standard.

Keywords: Motion capture, road cycling, kinematics, MVN, inertial systems

1. INTRODUCTION

1.1 Background

Motion capture (Mocap) is the process of measuring and digitally reproducing the motion of an object. Mocap of human movement involves individually tracking several strategic anatomical landmarks in space using motion sensors. These landmarks are used to estimate full-body kinematics using a biomechanical model consisting of several rigid body segments joined together by joints. The Mocap data can then be reviewed visually on a computer screen using an avatar or numerically for quantative analysis of segment kinematics and joint angles.

Mocap was first utilized in the 19th century, when it was employed in military programs to improve the mobility of troops [1]. However, it was only after the Second World War when there was a need for improved prosthetics and treatment for war veterans that the foundational studies were conducted in human locomotion by Eberhart and Inman [2]. Later, with the advent of computer processing, more sophisticated Mocap systems were developed. State-of-the-art Mocap systems, which utilize various different types of sensor technology, now provide full-body Mocap data in 3D and at sample speeds of several hundred and even thousand frames per second. Mocap is employed in a variety of fields today. For example, it is used in the entertainment industry for creating realistic animations in games and movies and for evaluating workplace ergonomics in industry [3]. It also provides accurate and comprehensive kinematic measurements for movement sciences research such as for gait analysis [4].

Optical Mocap systems such as the Vicon (Oxford Metrics Ltd.), which use advanced camera systems to track markers attached to the subject, are currently considered the gold-standard technology. However, due to significant advances made over the last two decades in the design and manufacture of micro-electromechanical systems (MEMS), an alternative Mocap technology has emerged: inertial Mocap systems (IMSs). IMSs track human motion using MEMS inertial measurement units (IMUs), which are compact sensor modules containing tiny accelerometers and gyroscopes, and magnetometers. IMU's are widely employed in inertial navigation systems (INSs) for aerospace, aviation, naval and ground transportation applications, as well as for robotics control. The major advantage of IMSs over the Vicon systems is their portability, since optical Mocap is generally restricted to laboratory use [5]. Furthermore, optical Mocap generally requires line of sight, good lighting conditions and significant post-processing [6]. IMSs are also significantly more affordable, quicker to set up and easier to use. However, one drawback of IMSs is that they are sensitive to prolonged magnetic interference, due to the use of magnetometers in the IMUs.

1.2 Motivation and objectives

Since optical systems have been the traditional benchmark in Mocap technology, almost all studies conducted using Mocap have been restricted to laboratory-based experiments. This has severely limited the scope of Mocap research performed in the field of sports science. However, for many sporting codes, IMSs are ideal for measuring an athlete's technique in their competitive arena instead of in a simulated laboratory environment. Therefore, the prospect of using an IMS for field-based Mocap holds great promise for more realistic experimental data. With insights gained from IMS field data, numerous improvements could be made to training

routines, injury prevention programs and performance optimization initiatives. However, although IMSs have already become extremely popular in the entertainment industry and have been validated for clinical studies [7, 8], they have not yet been readily adopted for sports science research. Therefore, the objective of this study was to determine the feasibility of using an IMS, the MVN BIOMECH system developed by Xsens B.V. (Enschede, Netherlands), to measure outdoor road cycling kinematics. The first potential obstacle which needed to be evaluated was measurement error caused by possible magnetic interference to the MVN from ferromagnetic materials in road bicycles.

2. DATA COLLECTION

2.1 The MVN BIOMECH system

The MVN system is stored in a portable suitcase, as shown in Figure 1a. It consists of 17 IMUs (Figure 1b), contained in a body-fitting Lycra suit (Figure 1c) which fixes the IMUs on strategic body segments to measure their individual kinematics. Two wireless onboard transmitters synchronize the IMU data signals and relay them to a nearby computer via USB receivers (Figure 1d). The MVN software then uses advanced sensor fusion techniques and a biomechanical model to digitally reproduce the full-body motion of the human subject. This is summarized in a whitepaper by Xsens [9].

Each IMU contains a triaxial accelerometer, gyroscope and magnetometer which together measure the IMU's global kinematics. The IMU data signals, which can be sampled at speeds ranging from 60-120 Hz, are used as inputs into an INS to track the motion of all 17 IMUs. Integration of the accelerometer and gyroscope measurements provides local linear and angular position, velocity and acceleration while the magnetometers are used as a compass to obtain heading in the global frame. Using pre-test calibration poses to obtain sensor-to-segment orientations the INS can then estimate the kinematics of an assigned rigid body segment for each IMU. The MVN software then assembles all the body segments together using a biomechanical model. The biomechanical model consists of 23 rigid segments connected by 22 joints, and is scaled anthropometrically to fit the physical dimensions of the test subject. By estimating the joint centre locations between the segments at each time step, the MVN system can then calculate the subject's full-body kinematics.

The MVN uses a recursive error-state Kalman filter to reduce measurement errors in the IMU sensors during the various stages of the Mocap process. In the INS, gyroscopic drift due to integration error is compensated for by the Kalman filter using sensor fusion. Drift in the horizontal plane is corrected using the heading data from the IMU magnetometers. Similarly, the accelerometers can be used as inclinometers to stabilize the gyroscopes in the vertical plane. Furthermore, accelerometer drift is addressed later in the biomechanical model using joint angle constraints and estimated contact points with the external world (such as feet on the ground). Lastly, advanced Kalman filtering is employed to reduce magnetic interference to the magnetometers caused by the close proximity of ferromagnetic materials or local magnetic fields. A more detailed treatment of the MVN operational principles is given by Roetenberg [10].

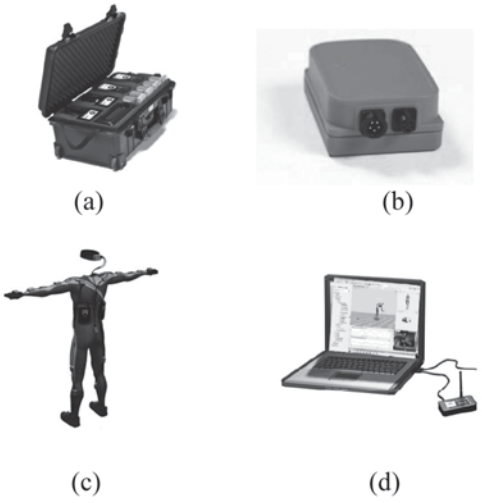

Figure 1: The MVN (a) suitcase (b) IMU (c) Lycra suit and (d) wireless transmitters and laptop (Source: Xsens)

2.2 Participants

Ten male cyclists were recruited for testing, all of which had competed regularly in professional races in the same season in which the testing was conducted. The cyclists used their own bicycles for the tests. Ethical approval was obtained for the testing and each subject granted informed consent to participate in the study.

2.3 Trial testing

The participants completed an indoor and outdoor test consisting of a one minute recording during steady state pedalling in a self-selected upright handlebar position at a constant cycling power of 3.5 $W.kg^{-1}$, which was used as an approximate medium intensity effort typical for competitive road cycling in another study [11]. The indoor test was conducted in a laboratory on a Powerbeam Pro stationary bicycle trainer (Figure 2a). The outdoor tests were conducted on a flat, straight stretch of open road (Figure 2b), with a pursuit vehicle carrying the laptop and receivers following within wireless range (~50 m). Each subject completed the tests on their own bicycle.

The basic sequence of the tests is shown in Figure 3. The suit setup included selecting the correct suit size and inserting and connecting the IMUs correctly. Secondly, the biomechanical model was scaled according to the subject's anthropometric dimensions. After this, the sensors-to-segment orientation was determined by the

two static calibration poses and two dynamic calibration movements. The subject then completed a warm up on the bicycle at 2 W.kg^{-1} for 3 minutes. Finally, the MVN recording was taken of the cyclist performing the test.

(a)

(b)

Figure 2: MVN recordings carried out (a) indoors on a trainer and (b) outdoors on the open road

After completing each recording, the MVN file was preprocessed in the MVN Studio software. This included reprocessing the file with the correct Kalman filter settings and editing the recording to isolate the desired period of the test. The raw magnetometer data for each IMU was then exported from the MVN software in XML format and imported into Matlab (Mathworks, Inc.) for data analysis.

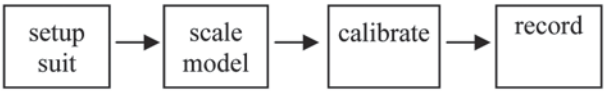

Figure 3: Main steps in test protocol

2.4 KiC benchmark test

Besides the default Kalman filter, which provides full-body kinematics without immunity to prolonged magnetic interference, the MVN system can also be operated with an alternative filter setting called Kinematic Coupling (KiC) [12]. The KiC algorithm calculates flexion angles for the hip, knee and ankle joints without the magnetometer data, making it immune to all magnetic disturbances. In order to evaluate the accuracy of the KiC data, a benchmark test was conducted with the gold-standard Vicon optical Mocap system. A single cyclist was recorded simultaneously with the MVN and Vicon systems (using the Plug-In Gait model) for one minute at 3.5 W.kg^{-1} on the Powerbeam trainer in order to compare the flexion measurements.

3. DATA ANALYSIS

3.1 Magnetic data

In order to evaluate the accuracy of MVN kinematic data it was necessary to quantify the magnetic interference caused by ferromagnetic bicycles components. This was done by determining the homogeneity of the local magnetic field measured by the IMUs. Two magnetic field parameters were used to do this. The first was the magnetic field intensity, which represents the density of the flux lines in the field. The second was the magnetic field inclination angle, which is the angle of the magnetic field relative to the global horizontal. The field intensity M_t was calculated for each IMU as in Equation 1.

$$|M_t| = \sqrt{m_{x,t^2} + m_{y,t^2} + m_{z,t^2}} \quad (1)$$

where $m_{x,t}$ $m_{y,t}$ and $m_{z,t}$ are normalized components of the magnetic field measurement within the local x-y-z coordinate system of each IMU's magnetometer. The scalar magnitude M_t was plotted as a function of time to identify changes in magnetic field intensity as a function of position for the moving IMUs on the lower limbs. Furthermore, intensity readings from stationary sensors on the upper body were compared to undisturbed field strength readings to determine the level of interference.

$$A_t = a_{x,t} + a_{y,t} + a_{z,t} \quad (2)$$

Similarly to the magnetometer data, the IMU accelerometer signal is represented by Equation 2. Since the inclination angle of the magnetic field is defined by the global horizontal, it therefore cannot be obtained directly from the IMUs local measurements because the orientation of the IMU in the global frame is unknown. However, when the IMU is stationary the accelerometer can be used as an inclinometer (by measuring the gravitational acceleration vector *g*) to determine the global vertical, and thus the perpendicular global horizontal, to rotate the IMU data measured in the local coordinate system to the global axis.

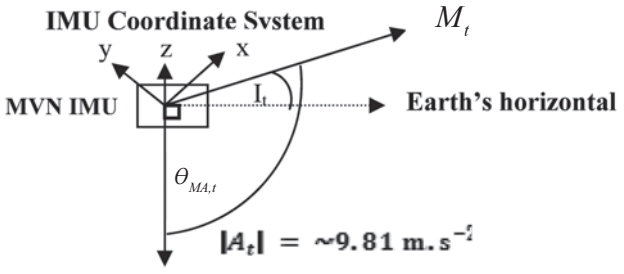

Figure 4: Inclination angle relative to M_t, A_t and the IMU

The angle between the magnetic field vector and gravitational acceleration vector can be calculated using the cosine rule as in Equation 3 (Figure 5).

$$\theta_{MA,t} = \cos^{-1}\left(\frac{|MA_t|^2-|M_t|^2-|A_t|^2}{-2|M_t||A_t|}\right) \quad (3)$$

where $|M|$ and $|A|$ represent the magnitude of the magnetic field intensity and approximate gravity vector respectively and are the two sides of the triangle adjacent to the angle $\theta_{MA,t}$.

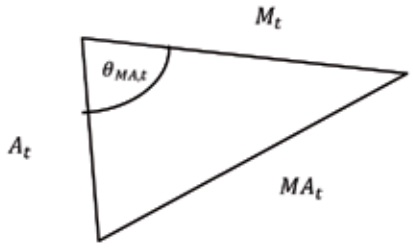

Figure 5: Cosine rule method used to calculate $\boldsymbol{\theta_{MA,t}}$

The third side of the triangle, $|MA_t|$, opposite to $\theta_{MA,t}$, represents the magnitude of the resultant vector of vectors A_t and M_t (Equation 4).

$$|MA_t| = \sqrt{(a_{x,t}-m_{x,t})^2+(a_{y,t}-m_{y,t})^2+(a_{z,t}-m_{z,t})^2} \quad (4)$$

Therefore, the inclination angle can be calculated as in Equation 5 because it is perpendicular to the angle $\theta_{MA,t}$.

$$I_t = \theta_{MA,t} - 90° \quad (5)$$

It should be noted that the inclination values calculated with this method are only approximate due to the estimation of the gravity vector using the accelerometers. Even with stationary IMUs, vibrations still occur during cycling which introduce error to the magnitude and direction of A_t when attempting to measure g. However, the method used here is sufficiently accurate for the purposes of identifying significant magnetic disturbances, especially since the noise on the A_t signal was found to be approximately Gaussian, with $|A_t|_{mean} \approx 10$ m.s^{-2}.

3.2 KiC data

The KiC algorithm calculates lower limb flexion angles (Figure 6) even in magnetically disturbed environments. In order to compare the KiC data with the Vicon data, it was necessary to ensure that the joint angle definitions were equivalent. For instance, although the knee functional axes are comparable, both hip angle definitions relied on different measurements of pelvic tilt. Therefore, in order for the hip data to be comparative the Vicon pelvic data was used for both data sets to calculate hip flexion. However, there was no known method for aligning the joint axes for the ankle. The sinusoidal flexion curves produced during the repetitive cycling motion were divided into separate pedal revolutions which were then interpolated and averaged to produce a single flexion curve for each joint representative of one pedal revolution during cycling.

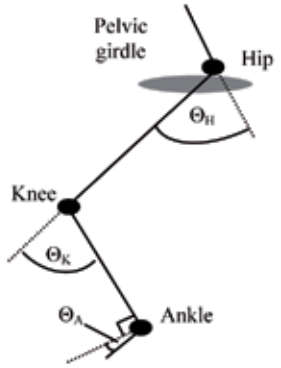

Figure 6: Definition of hip, knee and ankle flexion angles

4. RESULTS

Figure 7 shows the mean intensity readings taken during the MVN recordings by the lower limb segment IMUs for all ten cyclists. The undisturbed magnetic intensity (UI) in the geographical test location was measured at 50 (arbitrary unit) in a calibration test with a MVN IMU. As can be seen from the results, the outdoor environment was almost totally homogenous round the upper leg IMUs, with all mean outdoor values deviating less than 3% from UI. However, the indoor intensity was significantly offset from UI by an 8-10% bias error. Therefore, since this was a trend for all the IMUS during testing, it may be postulated that the indoor magnetic environment was distorted by laboratory-related factors such as ferromagnetic building materials and the indoor trainer used for the laboratory tests. Furthermore, the indoor and outdoor intensities were generally consistent during data collection (average deviations (ADs) were less than 2.5% of UI) as well as between cyclists.

On the other hand, the lower leg (shank) intensities showed a greater divergence between cyclists for both indoor and outdoor tests which suggests that these sensors were more affected by ferromagnetic materials on the bicycles. Moreover, the left shank was the most affected, with both indoor and outdoor intensities significantly higher. The general trend of decreasing homogeneity in the magnetic field, when moving closer to the pedals, was continued in the foot sensor measurements. Some pedal-foot interfaces, such as those for cyclists 5, 6 and 8, severely distorted the field intensity around the foot IMUs. Whereas the upper leg intensities were basically stable, the intensities near the feet varied on average by ~12% in the laboratory and

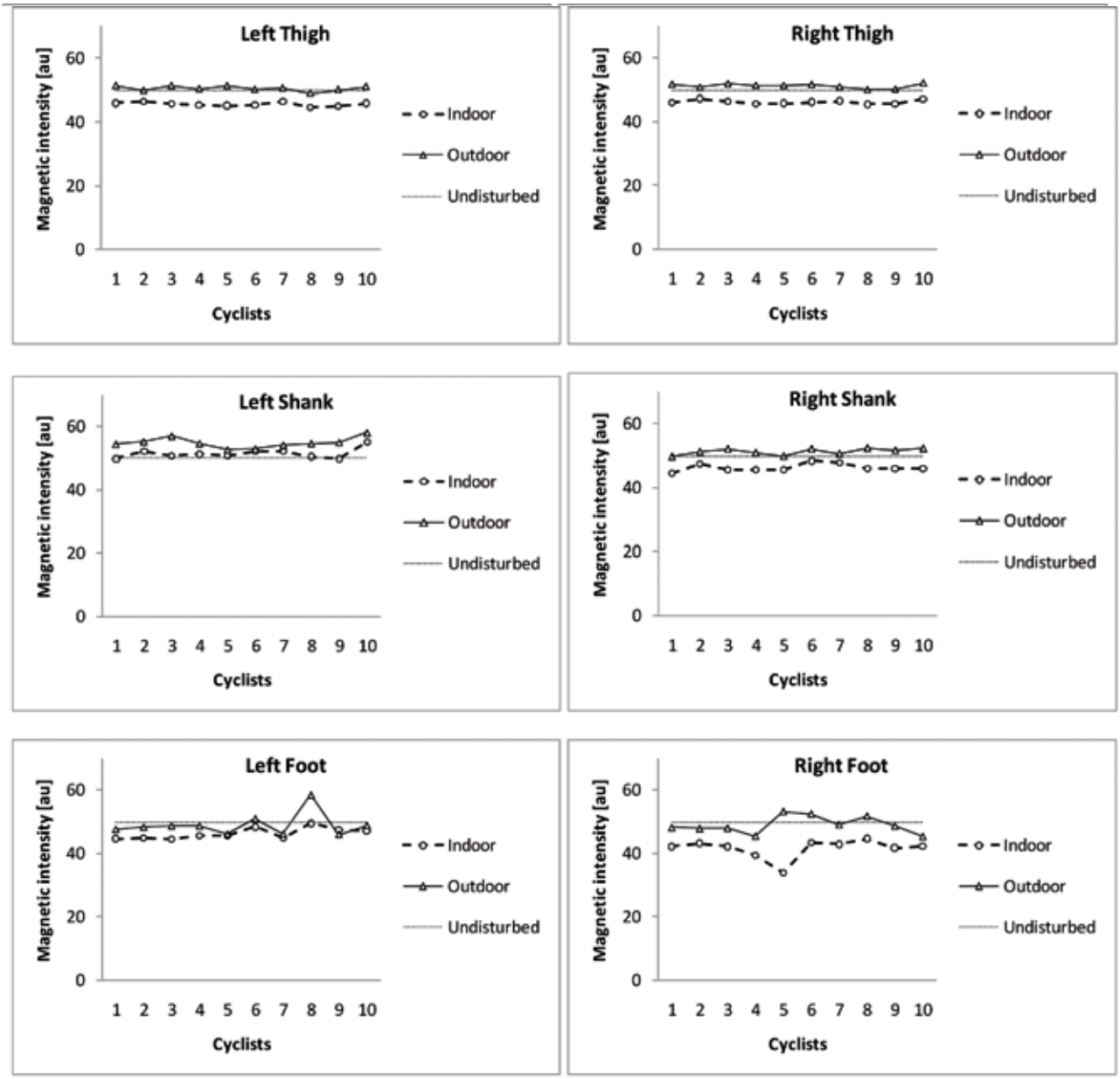

Figure 7: Magnetic field strength measurements for the three sensors on each cyclist's legs

~7% on the road. Some cyclists had disturbances of up to 39% for the left foot sensor.

Figure 8 presents the intensity measurements, as well as the indoor inclination values calculated for the stationary upper body IMUs. Interestingly, except for cyclist 2, results for the pelvic IMU show very little sign of magnetic interference in the seat area for all the cyclists. Similarly, the sternum IMU experienced no significant interference. However, both the sternum and the pelvic IMUs had large variances in their inclination angle values, which were caused by increased noise on the accelerometer signal due to oscillatory pelvic tilt and chest movement due to respiration. Predictably, the magnetic field closer to the handlebars was less homogenous. The left and right forearm sensors were considerably more disturbed than the sternum and upper arms. Even more so, the hands show highly erratic readings for both inclination angle and field strength.

The results from the KiC benchmark test are shown in Figure 9. The correlations between the MVN and Vicon measurements were high for all three joints (Table 1). The Θ_H values ($R^2 > 0.996$) were especially alike, with the root-mean-square error (RMSE) being smaller than 1° for both left and right hips. This is followed by Θ_K ($R^2 > 0.993$), which was still very similar to the Vicon. However, due to diverging measurements near maximum and minimum flexion the RMSEs were 3.4° and 3.1° for left and right legs respectively.

The correlations between measurements for Θ_A were slightly less high ($R^2 > 0.956$). The main reason for this was a significant offset of approximately 8° for the right ankle. The dashed black line represents the ankle flexion

after adjustment for the bias error. The flexion curves for Θ_A appear to have a very similar shape, especially during maximum dorsiflexion (Θ_{MIN}) at the beginning and end of the pedal stroke. However, as Θ_A increases into plantarflexion midway through the pedal stroke the Vicon curve is lower.

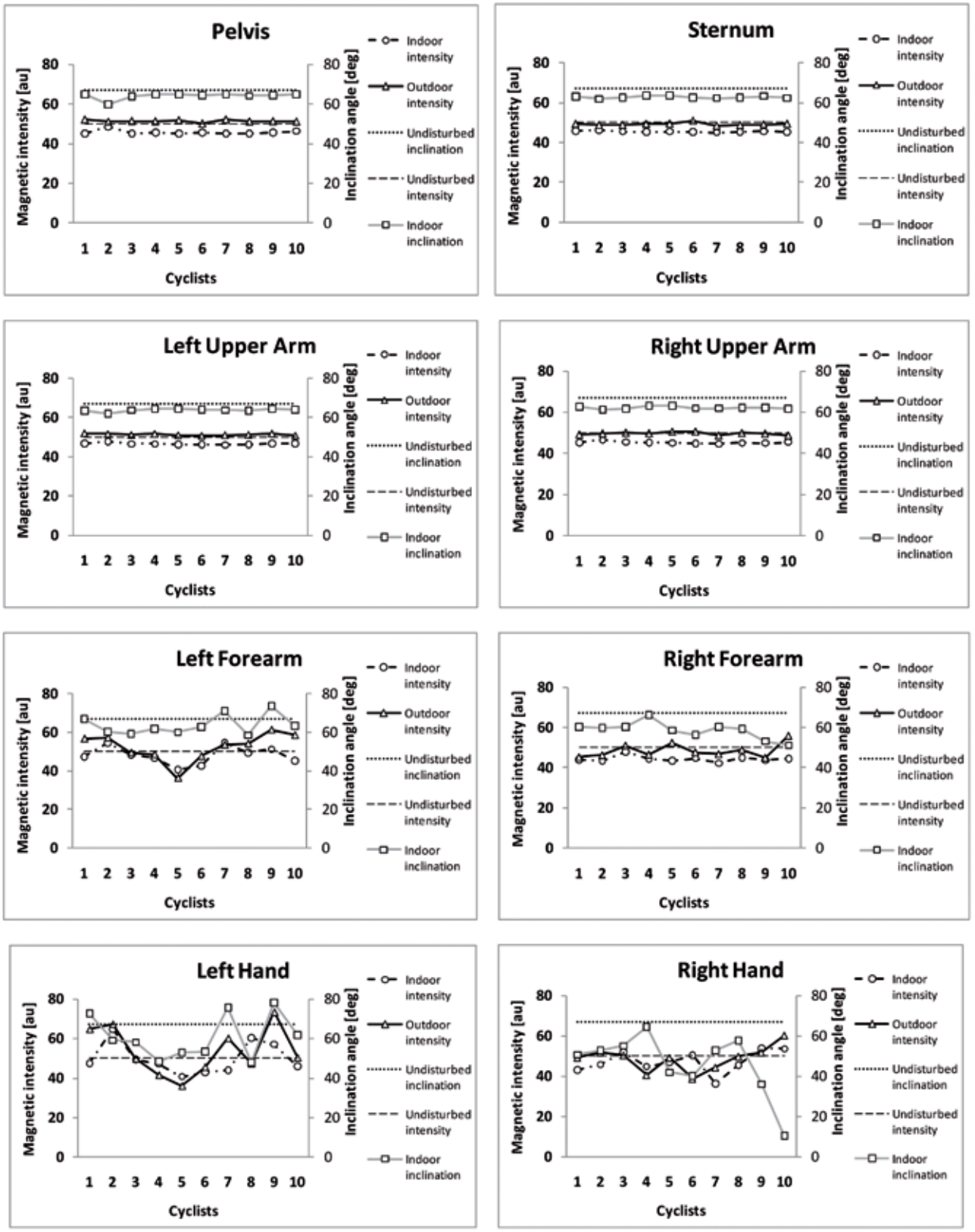

Figure 8: Magnetic field strength measurements for the pelvis, sternum, arm and hand segments

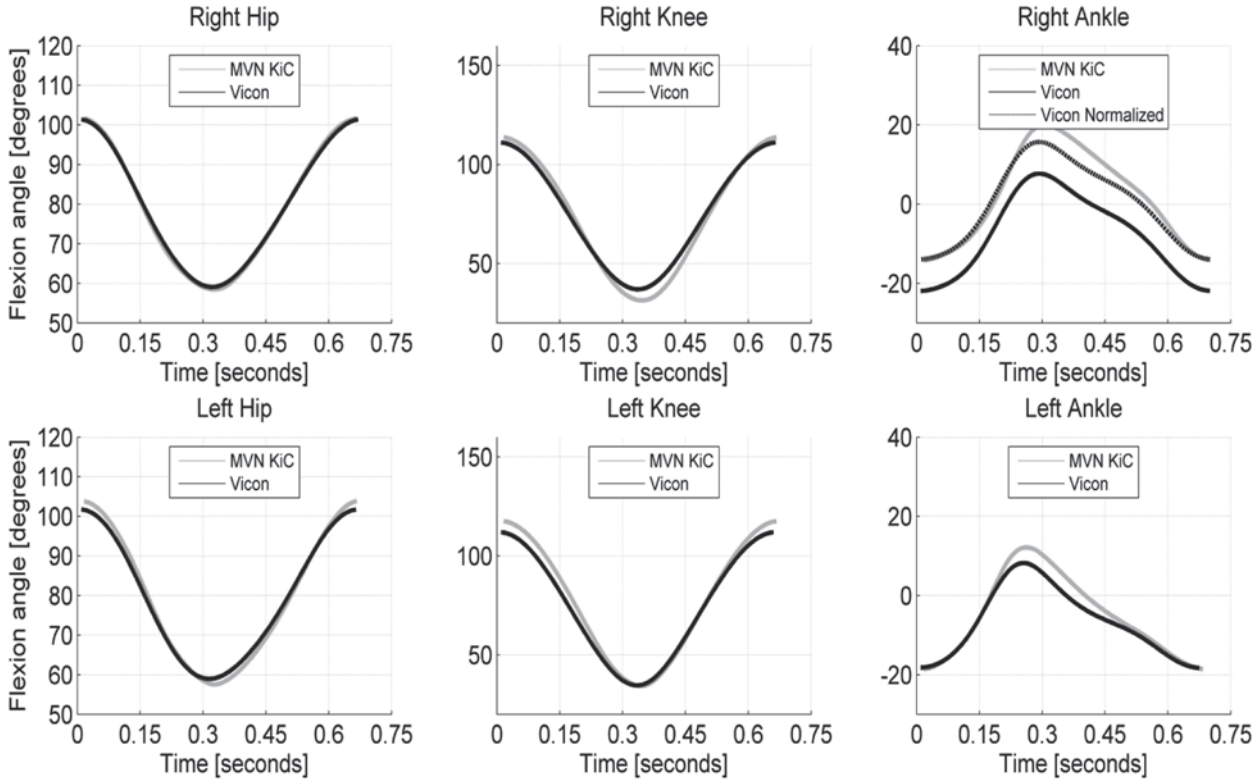

Figure 9: Comparison of right and left leg flexion measurements with Vicon and MVN KiC

Table 1: Benchmark test correlations and RMSE

	R^2	RMSE [°]
Hip [Left/Right]	0.996 / 0.997	0.9 / 0.8
Knee [Left/Right]	0.998 / 0.993	3.4 / 3.1
Ankle [Left/Right]	0.956 / 0.991	2.8 / 2.2

5. DISCUSSION

The interference to the magnetometer readings during the testing reduced the MVN Kalman filter's ability to compensate for gyroscopic drift error using sensor fusion. The resulting instability in the horizontal plane led to varied levels of degradation to the MVN biomechanical model. This was initially observed visually for the lower body in MVN Studio as an exaggerated hip abduction/adduction (due to drifting of the lower leg segment in the horizontal plane relative to the upper leg segment) and unrealistic ankle inversion/aversion (due to drifting of the foot segment relative to the lower leg segment). The disturbances to the arm sensors generally resulted in high uncertainties in the position of the shoulder joint centre and therefore also in the position of the hands segments and elbow and wrist joint angles.

The results of the magnetic analysis showed that the magnetometer measurements of many of the IMUs on the body segments furthest from the bicycle frame were not distorted. However, significant interference was evident in the data from the magnetometers near the handlebars and pedals (distal limb segments). Magnetic intensity levels deviated from the nominal value by an average of 10-15% for the hands and foot sensors, and as much as 50% in some cases. These disturbances are significant, especially when compared to a similar study done with the MVN IMUs on magnetic interference rejection methods, where a disturbance of more than 10% was considered large [13].

The relatively stable magnetic intensity measurements for the upper leg indicate a low level of bicycle-related interference around the hip area. The more disturbed magnetic fields measured around the tibial segment may be explained by the closer proximity of the lower leg sensors to ferromagnetic components such as the gear cogs, chain and other drivetrain elements. The erratic intensities measured by the foot sensors could again be due to different drivetrain materials, as well as metal screws in the cleats, metal clips in the pedals or (as is most probable) a combination of these factors. Although the sensors on the trunk of the subjects were minimally disturbed, the arm sensors showed increasing interference distally, similar to the leg sensors. This suggests that the pedal-foot and handlebar-hand interfaces were highly

disturbed for almost all cyclists due to ferromagnetic bicycle materials.

However, even though the normal MVN filter algorithm could not correctly measure cycling kinematics, the KiC algorithm can still be used to obtain some kinematic parameters despite the disturbances. Although the KiC algorithm performed very well during the validation test, some discrepancies were present between the inertial and optical systems' measurements. For instance, the MVN over-estimates knee extension in the right leg but not in the left. A possible reason for this may be leg length discrepancy, which is taken into account for the Vicon system by separate left and right leg segment measurements whereas the MVN model assumes bilateral symmetry in the biomechanical model. Therefore, these errors in segment length could translate into incorrect joint centre calculations and therefore 'false' or masked differences in left and right flexion. This is definitely a limitation when performing clinical measurements with the MVN, since there is no way to compensate for bilateral asymmetry in the test subject's anthropometry.

However, the difference for the ankle (a significant offset of approximately 8° for the right ankle) was definitely not due to asymmetry alone. The cause of this discrepancy is not known. However, the MVN data is assumed to be incorrect since the Vicon measured left and right ankles in the same region. It is highly likely that some form of experimental error occurred during marker placement. The similarity in the general shape of the curves suggests that the differences in ankle measurements with the Vicon, unlike the offset error for the right ankle, are related to differences in the processing of data for the biomechanical model for the two systems and not experimental error. It appears that the MVN measured ankle plantarflexion slightly high while measuring dorsiflexion very accurately. It is the opinion of the author that the main cause of the problems in the ankle measurement is that the rotational axes of this joint are defined differently in the MVN model to the Vicon model. However, although caution should be taken when interpreting Θ_A, the RMSE was still below 3° after adjustment for bias which is in fact very low.

6. CONCLUSION

The results of this study show that although professional road bicycles consist primarily of carbon-fibre and non-ferrous metals such as aluminium and titanium, they do in fact still cause significant interference to the MVN system when recording road cycling kinematics. Therefore, measurement of full-body kinematics is not yet possible for cycling with IMSs. However, the KiC algorithm does provide measurements of hip, knee and ankle flexion, which are important aspects in the analysis of road cycling technique and bicycle fitting, in hostile magnetic environments. Future work includes more rigorous testing of the KiC algorithm outdoors, as well as developing novel methods of filtering to remove the effect of the magnetic interference during outdoor road testing, with the aim of performing full-body outdoor assessment of cycling biomechanics.

7. REFERENCES

[1] Mündermann, L., Corazza, S. and Andriacchi, T.P. "The evolution of methods for the capture of human movement leading to markerless motion capture for biomechanical applications", *Journal of NeuroEngineering and Rehabilitation,* Vol. 3, 15 March 2006

[2] Eberhart, H. and Inman, V. "Fundamental studies of human locomotion and other information relating to design of artificial limbs" *Report to the National Research Council of the University of California,* 1947.

[3] Mavrikios, D; Karabatsou, V and Alexopoulos, K, et al. "An approach to human motion analysis and modelling", *International Journal of Industrial Ergonomics*, Vol. 36, pp. 979–989, 2006

[4] Cloete, T. "Benchmarking full-body inertial motion capture for clinical gait analysis". *University of Stellenbosch* : MSc thesis, 2008.

[5] Young, A. D., Ling, M. J., and Arvind, D. K. "Distributed estimation of linear acceleration for improved accuracy in wireless inertial motion capture" In *Information Processing in Sensor Networks, Proceedings of the 9th The International Conference in Sensor Networks* (2010), p. In press.

[6] A. Young, M. Ling, and D. K. Arvind, "Orient-2: A realtime wireless posture tracking system using local orientation estimation" in *Embedded networked sensors, Proceedings of the 4th workshop on ACM*, 2007, pp. 53-57.

[7] Cutti, A., Ferrari, A., Garofalo, P. *et al.* "'Outwalk': a protocol for clinical gait analysis based on inertial and magnetic sensors", *Medical and Biological Engineering and Computing,* Vol. 48, pp.17-25, 2010.

[8] Ferrari, A., Cutti, A., Garofalo, P. "First in vivo assessment of ''Outwalk'': a novel protocol for clinical gait analysis based on inertial and magnetic sensors", *Medical and Biological Engineering and Computing* Vol. 48, pp.1-15 .2010

[9] Roetenberg, D., Luinge, H. and Slycke, P. Xsens "MVN: Full 6DOF Human Motion Tracking Using Miniature Inertial Sensors" *Xsens Homepage.* [Online] 8 April 2009. [Cited: 10 January 2010.] http://www.xsens.com/images/stories/PDF/MVN_white_paper.pdf.

[10] Roetenberg, D. "Inertial and Magnetic Sensing of Human Motion" *Universiteit Twente, Netherlands*. PhD thesis, 2006

[11] Garcia-Lopez, J, et al. "Reference values and improvement of aerodynamic drag in professional cyclists", *Journal of Sports Sciences,* Vol. 3, pp. 277-286, 2008

[12] Garofalo, P. "Development of motion analysis protocols based on inertial sensors", *University of Bologna*, PhD thesis, 2010.

[13] Roetenberg, D., Luinge, H.J. and Baten, C.T. M. and Veltink, P.H. "Compensation of Magnetic Disturbances Improves Inertial and Magnetic Sensing of Human Body Segment Orientation" *IEEE Transactions On Neural Systems And Rehabilitation Engineering,* Vol.13. No. 3, September 2005